siRNA inhibition of endocytic pathways to characterise the cellular uptake mechanisms of folate functionalised glycol chitosan nanogels

*Paula Pereira[1], Sílvia S. Pedrosa[1], Jennifer M. Wymant[2], Edward Sayers[2], Alexandra Correia[3], Manuel Vilanova[3,4], Arwyn T. Jones[2], Francisco M. Gama[1]**

AUTHOR ADDRESS

[1]Institute for Biotechnology and Bioengineering (IBB), Centre of Biological Engineering, Campus de Gualtar, University of Minho,Braga, Portugal;

[2]Cardiff School of Pharmacy and Pharmaceutical Sciences, Redwood Building, Cardiff University, Cardiff, Wales CF10 3NB;

[3]IBMC - Institute of Molecular and Cell Biology, Rua Campo Alegre, 4099-003 Porto, Portugal.

[4]Abel Salazar Biomedical Sciences Institute, University of Porto, Rua de Jorge Viterbo Ferreira n° 228, Porto, 4050-313, Portugal;

KEYWORDS. Glycol chitosan nanogel, folate, siRNA transfection, endocytic pathways, intracellular localisation.

ABSTRACT. Glycol chitosan nanogels have been widely used in gene, drug and contrast agent delivery in an effort to improve disease diagnosis and treatment. Herein, we evaluate the internalisation mechanisms and intracellular fate of previously described glycol chitosan nanogels decorated with folate to target the folate receptor. Uptake of the folate decorated nanogel was impaired by free folate, suggesting competitive inhibition and shared internalisation mechanisms via the folate receptor. Nanogel uptake was shown to occur mainly through flotillin-1 and Cdc42-dependent endocytosis. This was determined by inhibition of uptake reduction observed upon siRNA depletion of these two proteins and the pathways that they regulate. The data also suggest the involvement of the actin cytoskeleton in nanogel uptake via macropinocytosis. After 7 h of incubation with HeLa cells, approximately half of the nanogel population was localised in endolysosomal compartments, while the remaining 50% of the material was in undefined regions of the cytoplasm. Glycol chitosan nanogels may thus have potential as drug delivery vectors for targeting different intracellular compartments.

1. Introduction

Macromolecular micelles, commonly termed nanogels, have been synthesised, characterised and studied for numerous biomedical applications including delivery of therapeutic entities. Active nanogel targeting strategies have been conceived to enhance their site-specific delivery by, for example, decorating the surface with ligands of plasma membrane receptors that are over-expressed on target cells [1].

A major advantage in the use of nanoparticles as drug delivery systems lies in their amenability to modifications that allow them to cross biological barriers. The cell membrane is naturally impermeable to complexes larger than 1 kDa, however, nanoparticle uptake may occur through a variety of active endocytic mechanisms, which depend on the physicochemical features of the

nanoparticle and the nature of the target cells. For the successful development of nanocarriers it is crucial to understand the molecular mechanisms involved in their interactions with the cell membrane, in addition to their entry via endocytic pathways and subsequent intracellular fate [2-4]. Generally, endocytosis can be divided into two broad categories: phagocytosis (uptake of large particles) and pinocytosis (uptake of fluids, solutes and also ligands via plasma membrane receptors). Phagocytosis is characteristic of specialised professional phagocytes, while pinocytosis is present in virtually all cells and has multiple forms depending on the cell origin and function [5]. Several different classifications for pinocytosis have been proposed, and a common approach is to order according to the key proteins involved: clathrin-mediated endocytosis (CME), caveolae-mediated endocytosis (CvME), clathrin- and caveolae-independent endocytosis and macropinocytosis. Clathrin- and caveolae-independent pathways can be further sub-classified as Arf6-dependent, flotillin-1-dependent, Cdc42-dependent and RhoA-dependent endocytosis [5-9].

The uptake mechanism of a drug delivery system is likely to influence its intracellular fate and capacity to mediate a biological response. The aim of the present study was to identify the endocytic mechanisms responsible for the internalisation of glycol chitosan nanogels functionalised with folate in HeLa (cervical adenocarcinoma) cells that overexpress folate receptors [10]. Conventionally, chemical endocytosis inhibitors have been used to analyse cellular uptake of drug delivery vectors including chitosan nanoparticles, but these inhibitors are associated with problems related to toxicity and low specificity– [11-13]. Selective inhibition of different endocytic pathways can also be attempted by siRNA-targeting and subsequent depletion of key proteins that orchestrate individual pathways [14, 15].

In this work, single siRNA sequences were used to attenuate pathways regulated by clathrin heavy chain (si-CHC), caveolin-1 (si-Cav-1), p21-activated kinase 1 (si-Pak-1), Flotillin-1 (si-Flot-1) [14] and Cdc42 (si-Cdc42). These cells were then used to determine the mechanism of uptake and intracellular fate of the nanogels to provide valuable information regarding their capacity to deliver different types of cargos.

2. Experimental

2.1. Reagents

Glycol Chitosan (GC, G7753), mercapto hexadecanoic acid (MHDA), N-hydroxysulfosuccinimide (NHS), 1-Ethyl-3-[3-dimethylaminopropyl]carbodiimide hydrochloride (EDC), O-methyl-O'-succinylpolyethyene glycol 2000 (PEG2000), O-(2-Aminoethyl)-O'-(2-carboxyethyl)polyethylene glycol 3000 hydrochloride (PEG3000), folate, 3-(4,5-dimethylthiazol-2-yl)-2,5-diphenyl tetrazolium bromide (MTT) and sulforhodamine B (SRB) were purchased from Sigma (St. Louis, MO, US). Folate-free RPMI 1640 medium, Opti-MEM, oligofectamine, Alexa Fluor® 647 Dextran 10.000 MW (Alexa647-Dextran), Alexa Fluor® 647 transferrin (Alexa647-transferrin), Alexa Fluor® 488 carboxylic acid (succinimidyl ester) were bought from Invitrogen (Carlsbad, CA, USA). Complete mini protease inhibitor cocktail tablets were from Roche Diagnostics (Mannheim, Germany). Single siRNA sequences of 21-23 residues were acquired from Europhins MWG Operon (Ebesburg, Germany) as previously described [14].

2.2. Antibodies

Antibodies recognizing Clathrin Heavy Chain was from NeoMarker (California, US); Anti-Cav-1 was from Cell signalling Technology (Hertfordishire, UK); Anti-Pak-1 was from Cell Signaling (Danvers, Massachusetts, US) and antibody to Flot-1 was from BD Bioscience (Oxford, UK); Anti-γ-tubulin was from Sigma (Dorset, UK). Secondary goat anti-mouse- and goat anti-rabbit- HRP were from Pierce (Loughborough, UK).

2.3. Cell culture

HeLa cancer cells were cultured in DMEM supplemented with 10 % foetal bovine serum (FBS), 100 IU/mL penicillin and 0.1 mg/mL streptomycin. The cells were maintained as a subconfluent monolayer in a humidified atmosphere containing 5 % CO_2 at 37 ºC.

2.4. Self-assembly of nanogels

Details of Glycol Chitosan nanogel synthesis and characterisation as folic acid functionalised nanogels were described in a previous report[16]. Briefly: nanogel synthesis was performed in two independent steps. Initially, folate is conjugated to PEG3000 (FA-PEG3000). In the second reaction, FA-PEG3000, PEG2000 and MHDA were grafted onto the GC polymer. The nanogel dispersions used in the different experiments were obtained after dispersing the lyophilised reaction product in distilled water, under magnetic stirring at 50 ºC for 48 h, and passing through a pore size 0.45 μm cellulose acetate syringe filter.

2.5. Preparation of the Alexa Fluor® 488 labelled nanogel

The nanogels were labelled with Alexa Fluor® 488 carboxylic acid (succinimidyl ester) through an amide linkage. The Alexa488 was dissolved in DMSO. The molar ratio of Alexa488

carboxylic groups to the nanogel free amine groups was 0.11. The dye was added to nanogel dispersions at 1 mg/mL in PBS and incubated in the dark at room temperature for 24 h. Thereafter, the reaction mixture was extensively dialysed (MW cutoff 10-12 kDa) against distilled water to remove free Alexa488. To verify the absence of free dye, the conjugated Alexa488-nanogel was purified by centrifugation at 3,000 x g through a 10 kDa MW cut-off filter.

2.6. Cellular uptake of nanogels by flow cytometry

HeLa cells were seeded onto 24-well plates at $2.0x10^5$ cells per well and left to adhere overnight. The cells were treated with nanogels at 0.2 and 0.4 mg/mL for 0, 1, 3, 7 and 24 h. After each time point the mixture, the culture medium and nanogels suspensions were removed and the cells were washed with PBS and collected using 150 μL of trypsin/EDTA (0.25%/0.02%) in PBS 2 min at 37 ºC; after addition of FBS supplemented medium the cell suspension was centrifuged at 300 x g for 10 min and rinsed with PBS. The cell associated fluorescence was measured by flow cytometry using a Coulter Epics XL Flow Cytometer (Beckman Coulter Inc., Miami, FL, USA).

2.7. siRNA transfection

The transfections were performed as described by Soraj *et al*. [14]. Briefly: cells were seeded in antibiotic-free medium at a density of $1.6x10^5$ cells in a 35 mm glass bottomed imaging dish (MatTek, Ashland, USA) and per well in a 6-well plate. For 12-well plates the density was reduced to $6.7x10^4$ cells per well. The cells were cultured overnight to obtain the desirable confluency at the beginning of the transfection (~60%). The siRNA transfection procedure was adjusted according to well diameter. Volumes used for a 12-well plate were: 0.5 μL of 50 μM of

stock siRNA diluted in 89.5 µL of Opti-MEM and 2.0 µL of oligofectamine in 8.0 µL of Opti-MEM. The diluted solutions were then gently mixed and stored at room temperature for 30 min. For each well, the media was removed and replaced with 400 µL of Opti-MEM. The complex siRNA-oligofectamine was added dropwise to the wells and incubated at 37 ºC and 5 % CO_2 for 4 h. Thereafter 250 µL of Opti-MEM containing 30 % (v/v) of FBS was added to the transfection mixture and the cells were incubated under tissue culture conditions for 48 h.

2.8. *In vitro* viability of the transfected cells

MTT assay

The effect of siRNA transfection on cell metabolic activity was evaluated using the quantitative colorimetric MTT assay. The cells were seeded onto 24-well cell culture plates at a density of $3.4x10^4$ cells per well and transfected with the different siRNAs as described above. After the transfection period (48 h) cell metabolic activity was measured by adding MTT (3-(4,5-dimethylthiazol-2-yl)-2,5-diphenyl tetrazolium bromide) [17]. The MTT solution (0.5 mg/mL in PBS) was carefully removed from each well and the resulting dark blue formazan crystals were solubilised in dimethyl sulfoxide and quantified spectrophotometrically at 570 nm. A reference absorbance at 690 nm was measured for the purposes of background subtraction.

Sulforhodamine B assay

Cell proliferation of the siRNA transfected cells was assessed using the Sulforhodamine B (SRB) assay, which provides an estimate of total protein which in turn is related to cell number [18, 19]. After transfecting cells with siRNAs for 48 h, 24-well plates were rinsed with PBS and left to dry at 37 ºC, 5 % CO_2. Ice cold 1% acetic acid: 100% methanol solution was then used to fix the

cells at -20 ºC for 30 min. After discarding the fixative solution the plates were left dry at 37 ºC before adding 250 µL of 0.5 % of SRB in 1 % acetic acid to each well. Ninety minutes later the cells were 4x washed with 1 % of acetic acid to remove the excess Sulforhodamine B and then left dry. 1.0 mL of 10 mM Tris solution was used to dissolve the Sulforhodamine. The supernatant was used for quantification of SRB protein staining that was quantified by a spectrophotometer at 540 nm.

2.9. Nanogel internalisation in endocytosis compromised cells

2.9.1. Fluorescence microscopy

Live cell imaging via confocal microscopy

siRNA-transfected cells, 48 h post transfection (Section 2.7) in glass-bottomed 35 mm culture dishes were incubated with nanogels at 0.2 mg/mL for 7 h. The cells were then rinsed extensively with PBS and immediately imaged as live cells in phenol red free-DMEM by confocal microscopy at 37 ºC on a Leica SP5 system, as previously described [14]. Control and CHC depleted cells, were also incubated for 16 min with the CME probe Alexa647-transferrin (50 nM) to evaluate the efficiency of transfection.

Immnunolabelling

Cav-1 depletion was confirmed by immunolabelling and confocal microscopy. At the end of the transfection the cells on glass coverslips were rinsed with PBS and fixed with 3 % PFA for 15 min at room temperature. Then the samples were treated with 50 mM of PBS/NH_4 for 10 min to quench reactive species resulting from fixation. After 3x PBS washing the cells were permeabilised with PBS/0.2 % Triton X-100, washed and immersed in blocking buffer, 2 % (v/v)

foetal calf serum and 2 % (w/v) BSA in PBS, for 30 min. Cells were then incubated with the primary antibody recognizing Cav-1 and subsequently with secondary Alexa546 labelled antibody. The cells were finally incubated in Hoechst 33342 for 10 min at room temperature to label the nucleus. Finally, the coverslips were mounted on glass sides and the cells were visualised by confocal microscopy. Cells were imaged through the z-axis to generate z-projection images.

2.9.2. Flow cytometry

Quantification of cell associated fluorescence in siRNA transfected cells following incubation with nanogel was performed by flow cytometry. For this, siRNA transfected cells in a 12-well plate were incubated with Alexa488-nanogel (0.2 mg/mL) for 7 h under tissue culture conditions. The cells were then thoroughly washed with PBS, trypsinised with trypsin/EDTA 0.25%/0.02% in PBS for 2 min at 37ºC; after addition of FBS supplemented medium the cell suspension was centrifuged at 300 x g for 10 min. The cell suspension was washed with PBS. Cell-associated fluorescence of the cell suspension was measured using a Coulter Epics XL Flow Cytometer (Beckman Coulter Inc., Miami, FL, USA).

2.9.3. SDS page and Western blotting

Following 48 h of siRNA transfection, the cells from 6 well plates were washed in ice-cold PBS and collected on ice by scraping in 100 µL of lysis buffer (50 mM Tris-HCl, 150 mM NaCl, pH 8.0, 1 % Triton X-100), containing protease inhibitor cocktail. Lysates were then centrifuged at 13,000 x g (4 ºC) for 10 min before adding three parts supernatant to one part 4x Laemmli buffer. The samples were heated at 95 ºC for 5 min and centrifuged at 13,000 x g (4 ºC) for 1

min prior to loading (18 μg of protein per well) onto 10 % acrylamide gels for separation by SDS-PAGE. Following electrophoresis the separated proteins were transferred to PVDF membranes that were rinsed with PBS and blocked in 5 % milk in PBS Tween 20 (0.025%; PBST) for 1 h. The membranes were then probed with antibodies recognising CHC, Cav-1, Pak-1, Flot-1, γ-tubulin and β-actin diluted in 2 % milk in PBST. Following washing in PBST, species specific secondary antibodies conjugated to horseradish peroxidase (HRP) and diluted in 2 % milk in PBST were applied to the membrane. Protein bands were detected by Enhanced Chemiluminescence (ECL).

2.10. Nanogel intracellular localisation

HeLa cells were seeded at $3x10^5$ cells in glass bottom dishes and left to adhere overnight. 0.2 mg/mL of the Alexa488-nanogel and 0.025 mg/mL of Alexa647-Dextran were then co-incubated with cells for 7 h in folic acid free medium. In the case of Alexa488-nanogels co-incubation with Alexa647- transferrin (50 nM) was performed by adding transferrin 16 min before the end of the nanogel incubation period (7 h). The cells were extensively rinsed with PBS and immediately imaged as live cells in phenol red free-DMEM by confocal microscope at 37 ºC.

2.11. Statistical analysis

Results are expressed as mean ± S.D. of three independent experiments, each one with n=3. Statistical significances were determined by applying a one-way ANOVA with a Dunnett's Multiple comparison test through Prism software (GraphPad software version 5.00, USA). Significance of the results is indicated according to p values * $p<0.05$, ** $p<0.005$ and *** $p<0.0001$.

3. Results and Discussion

We have previously shown folate functionalised glycol-chitosan nanogel have increased uptake over the unfunctionalised nanogels [16]. Herein we investigate the uptake and internalisation properties of the folate functionalised nanogels.

3.1. Cellular uptake of nanogels as a function of time, concentration and presence of folate

We examined the effects of folic acid functionalised nanogel concentration and the presence of folate in the culture medium on the internalisation of Alexa488-nanogel at different time points. HeLa cells were incubated for different time periods with the fluorescent nanogels at concentrations of 0.2 and 0.4 mg/mL in media either depleted of, or containing folate. Cells were collected and the mean fluorescence intensity (a proxy for nanogel uptake) was measured by flow cytometry.

Figure 1 (A) shows that nanogel uptake increases with time over a 24 hour period in cells incubated with 0.4 mg/mL nanogel. However, in cells incubated with 0.2 mg/mL nanogel, uptake increases over the first 7 h but then at some time during the 7-24 h incubation period the mean fluorescence intensity decreases. The data indicate not only reduced uptake at this lower concentration but also a loss of the nanogel from the cells. This suggests that during longer incubation periods (7 h+) at this concentration the fluorescently labelled nanogel may either be recycled out of the cell or degraded. Degradation would seem more likely as recycling would potentially lead to reuptake of the nanogel and as such we would expect to see stabilisation in the level of internalised nanogel rather than loss.

Figure 1B demonstrates that internalisation of the Alexa488-nanogel is significantly increased in folate-depleted culture conditions compared with culture in normal media. The presence of free folate in the culture medium has previously been shown to lead to a decrease in uptake of folate-conjugated nanoparticles by cells overexpressing folate receptors [7, 20]. Viewed in this context we suggest that the folate receptors may be involved in the internalisation of the Alexa488-nanogel, although other non-specific mechanisms may also contribute to the uptake. To eliminate the inhibitory and potentially confounding effects of folate in the media, folate was eliminated from subsequent uptake experiments.

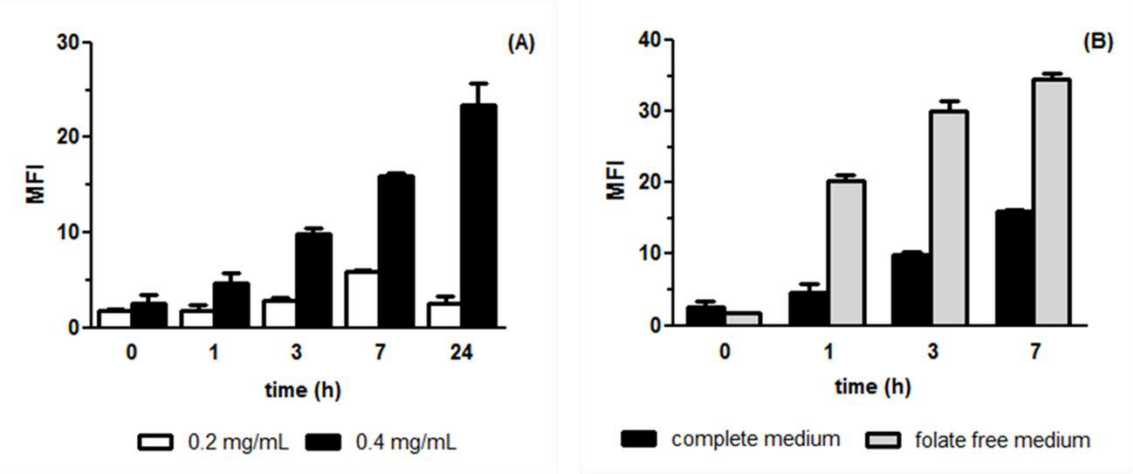

Figure 1. Effects of nanogel concentration (A) and the presence of folate in the culture medium (B) on the internalisation of Alexa488-nanogel at different time points in HeLa cells. Mean fluorescence intensity (MFI) was used as a proxy for fluorescent nanogel uptake and was measured by flow cytometry at various time points up to 24 h (A) and 7 h (B).

3.2. Inhibition of endocytic pathways through siRNA depletion of endocytic proteins

3.2.1. Viability of siRNA-transfected cells

The mechanism of nanogel internalisation was studied using siRNA transfection as a tool to silence endocytic proteins and inhibit distinct endocytic pathways. It is known that the level of

cellular toxicity caused by transfection is dependent on the reagent used and on the nature of the cells. Cell proliferation and metabolic activity of HeLa cells transfected using oligofectamine were studied to ensure that the viability was not compromised by the procedure. The metabolic activity of HeLa cells was not significantly affected by transfection (Figure 2, A). Although statistically significant differences were detected in total protein levels, these are relatively small and unlikely to be of biological significance (Figure 2, B).

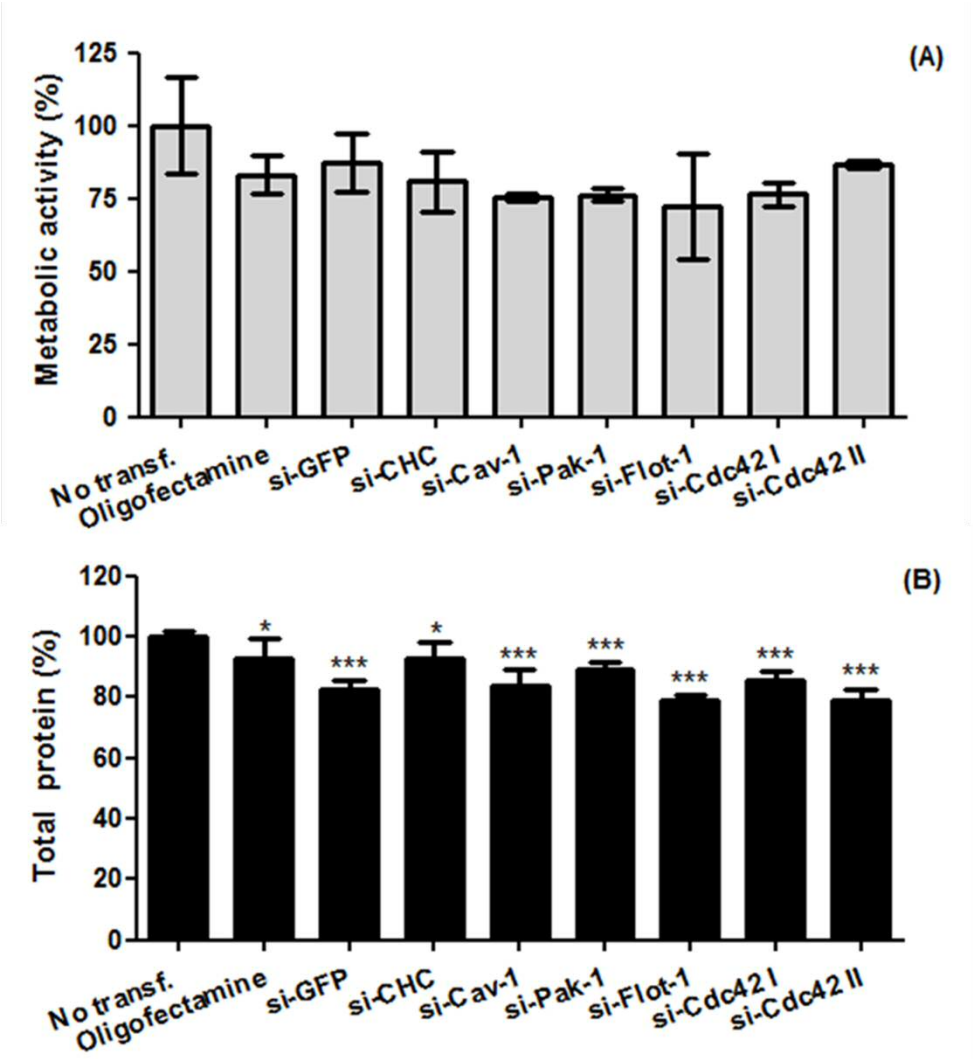

Figure 2. Effect of the si-RNA transfection on metabolic activity and total protein mass of HeLa cells assed by the MTT (A) and sulforhodamine (B) assays. * $p<0.05$ or *** $p<0.001$ represent

the statistical significance of differences in viability between non-transfected cells and the siRNA depleted samples. The results were expressed as mean ± SD.

3.2.2. Cellular uptake mechanism(s) of the nanogels by endocytosis compromised cells

Inhibition of clathrin mediated endocytosis (CME)

Clathrin-mediated endocytosis (CME) is the best characterised mechanism of endocytosis and requires the Adaptor-2 complex in association with clathrin heavy and light chain [7, 8]. Cargos taken up by clathrin-coated vesicles follow the classical endocytic pathway to early endosomes where sorting occurs for delivery to other organelles such as the lysosomes or back to the cell surface through recycling endosomes[13]. The uptake and recycling of transferrin occurs through this endocytic pathway, hence this protein is commonly used as a marker to detect interference with CME [14, 21]. CHC is the major coat protein associated to this internalisation pathway [7]; thus in the present study si-CHC transfected HeLa cells were incubated with Alexa647-transferrin to evaluate the efficiency of CME inhibition. Transferrin uptake in clathrin depleted cells was visibly lower compared with non-transfected and si-GFP transfected cells (Figure 3, A), reflecting successful and population-wide transfection. CHC depletion was directly confirmed through CHC expression analyses in cell lysates (Figure 3, B). In order to ascertain if the nanogel utilises this internalisation pathway, si-CHC transfected HeLa cells and the respective controls were incubated with nanogels and then analysed via confocal microscopy (Supplementary Figure 1) and flow cytometry (Figure 3, C) revealed no differences in nanogel uptake between control cells and those deficient in CME suggesting that this pathway is not involved in nanogel uptake.

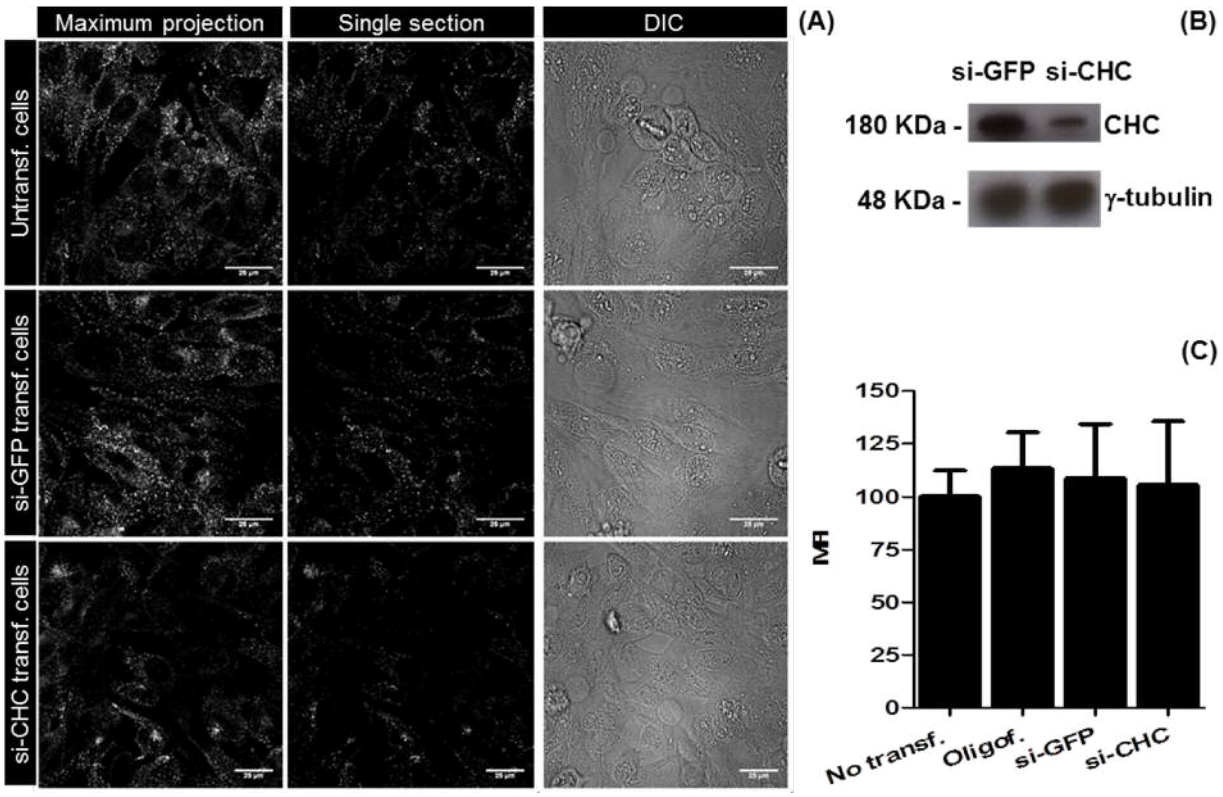

Figure 3. CME inhibition in HeLa cells. (A) Confocal visualisation of HeLa cells transfected with si-CHC or si-GFP control for 48 h prior to incubation with Alexa647-transferrin for 16 min. For each condition (rows) the images correspond to (left to right) maximum projection, middle z section through the cells and Differential Interference Contrast (DIC) images. The scale bars represent 25 μm. (B) CHC expression after transfecting HeLa cells with si-CHC for 48 h. (C) Effect of the CME silencing on nanogel cellular uptake expressed as mean fluorescence intensity (MFI). Error bars represent S.D.

Inhibition of caveolae-mediated endocytosis (CvME)

CvME starts with the formation of caveolae on the plasma membrane of cells, often in lipid rafts. Caveolae are noted as being enriched in the protein Cav-1 and have a diameter between 50-100 nm. A dynamin dependent scission of the caveolae from the membrane then results in the

formation of the endosome-like caveosome [8]. Initially the caveosome interior was thought not to acidify to any great extent with delivery of cargo to the Golgi and/or endoplasmic reticulum, thus avoiding the lysosomal degradation [8]. However, Chiu *et al*. [22] revealed that N-palmitoyl chitosan nanoparticles enter cells via caveolae and were transiently localised in caveosomes before trafficking to the canonical endosomal pathway en route to lysosomes. Agents, such as viruses, that are taken up by caveolae are also thought to end up in endosomes that can be directed to lysosomes. Evidence from electron microscopy studies suggest that caveosomes represent a special type of caveolar endosome that always associates with the plasma membrane [23]. The theory behind the existence of caveosomes mostly results from studies which involve caveolin overexpression or caveolin mutants and as such may or may not be a naturally occurring phenomenon [23].

CvME inhibition was achieved through depletion of Cav-1 using transfection with si-Cav-1. Since Cav-1 is a critical component of caveolae formation at the plasma membrane [8],its depletion results in the impairment of CvME. The efficiency of siRNA transfection was visualised by immunofluorescence microscopy of Cav-1, since a reliable endocytic marker equivalent to transferrin for CME, for assessing uptake via caveolae has not yet been identified. As shown in Figure 4 (A) a decrease in caveolin vesicle labelling was clearly observed in si-Cav-1 transfected cells. Significant Cav-1 depletion was also confirmed through Western blot analysis of cell lysates (Figure 4, B).

There is data to suggest that folate internalisation through the folate receptor occurs via CvME [3]. For example, folate-targeted poly(ethylene glycol) (PEG)-coated nanoparticles were thought to internalise via caveolae-assisted endocytosis and the nanoparticles were subsequently visualised in punctate structures [24]. Conversely, internalisation and trafficking of folate receptors was found

not to be exclusively caveolae dependent: specifically, folate-protein conjugates after binding to folate receptors on the surface of cancer cells, irrespective of size, were internalised via uncoated pits or caveolae, however at later times (6 hours), some conjugates were found in lysosomes; so caveolae-mediated endocytic pathway converged with a pathway utilised by clathrin-coated pits. [25]. In agreement with this, as shown by confocal microscopy in supplementary Figure 2 and quantified by flow cytometry in Figure 4 (C), nanogel uptake was reduced, but not significantly ($p \geq 0.05$), in Cav-1 depleted cells. However, it should be noted that when a particular route is inhibited others may become activated as a compensatory mechanism [22]. For example, Cav-1 depletion has been shown to result in increased levels of activated Cdc42 at the plasma membrane [5]; this protein is thought to regulate the actin cytoskeleton and folate internalisation through the glycosylphosphatidylinositol (GPI)-anchored folate receptor [26].

The hydrophobicity of the cargo may be a determining factor for its internalisation via CvME. The uptake of N-palmitoyl chitosan nanoparticles was associated with lipid raft-mediated endocytic routes, and substitution of chitosan with a higher level palmitoyl groups (>10 %) increased the fraction of nanogel uptake via CvME [22].

Also noteworthy is the impact of nanogel size distribution on CvME and indeed on other pathways. The nanogels in this study have mean diameters of around 200 nm and size may play a critical role in their mechanism of uptake. To our knowledge no studies have unambiguously demonstrated that caveolae can accommodate particles larger than 100 nm and this has previously been noted [27]. However, CvME was thought to play a major role in the cellular uptake of Chitosan/DNA/poly(γ-glutamic acid) complexes with an average size of approximately 150 nm [28]. It should be noted that most studies suggesting that caveolae are involved in the uptake of

drug delivery vectors rely on the use of chemical endocytosis inhibitors, which often influence more than one pathway[12].

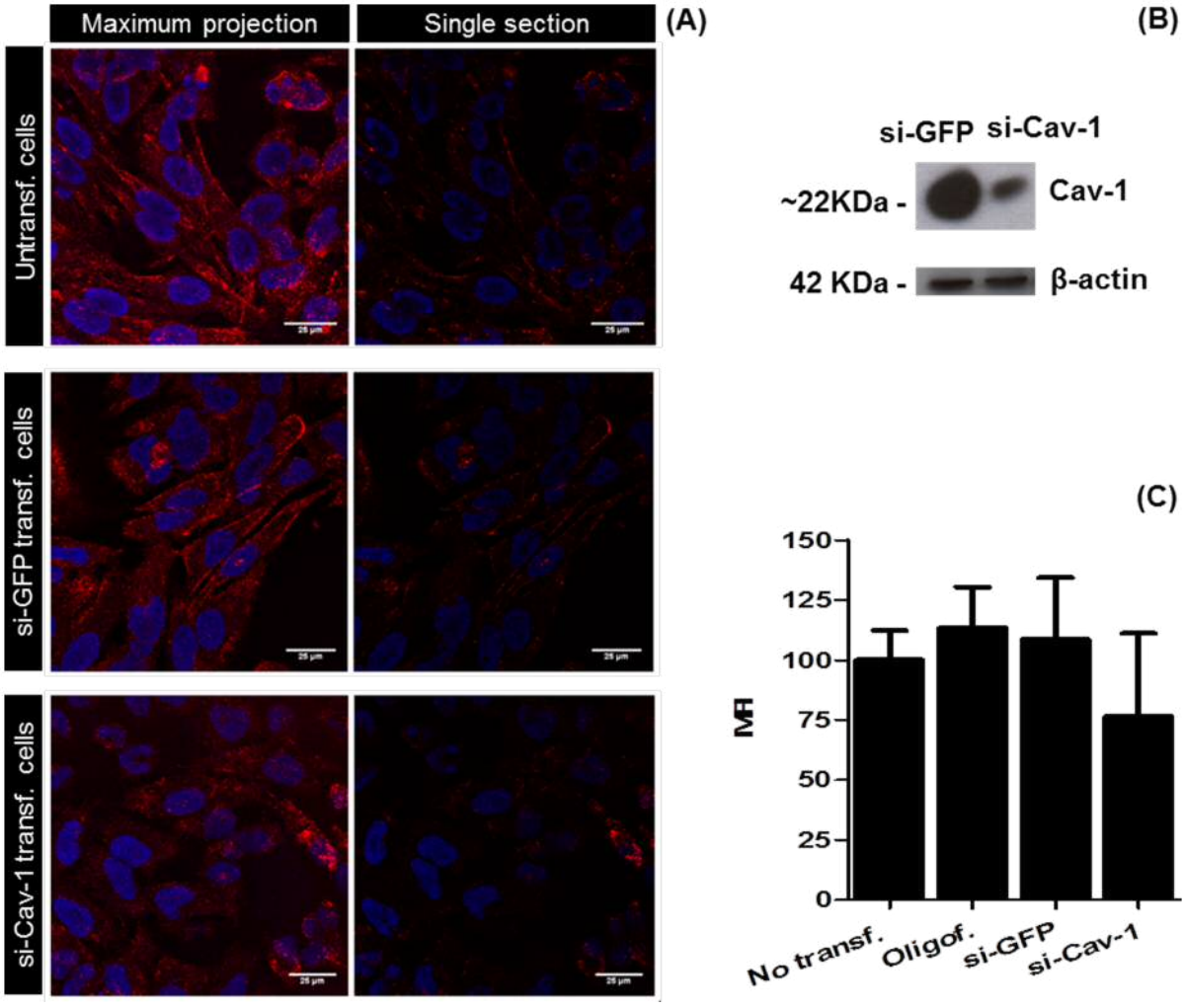

Figure 4. CvME inhibition in HeLa cells. (A) Control and si-Cav-1 or GFP treated cells, were fixed after 48 h, labelled with antibodies against Cav-1 and Alexa546 conjugated secondary antibody and then analysed by confocal fluorescence microscopy. Maximum projection (left) and a single z section (right) is shown to each condition; nuclei are labelled with Hoechst 33342. Scale bars represent 25 μm. (B) Cav-1 expression after transfecting HeLa cells with si-Cav-1 for 48 h. (C) Effect of the CvME inhibition on cellular uptake of nanogels expressed as mean fluorescence intensity (MFI). Error bars represent S.D.

Inhibition of macropinocytosis

Macropinocytosis is a poorly characterised pathway that internalises extracellular material in the fluid-phase. This process involves, especially after growth factor activation, membrane ruffling and formation of relatively large vesicles, named macropinosomes. These are heterogeneous in size, generally considered larger than 0.2 μm and have no clearly identified and unique coat structures [29, 30]. It is known that p21-activated kinase (Pak-1) is associated with growth factor induced macropinosomes [14] and can be activated by the small GTPases Cdc42 and Rac1 [31]. Whether the fate of macropinosomes inside the cells involves fusion with lysosomes or recycling to the plasma membrane, or a mixture of both, is unclear, and likely to be dependent on cell type [8].

The addition of cationic molecules and particles to cells will inevitably result in interaction with the negative surface mediated by surface sugars [2, 3]. This may or may not lead to internalisation via membrane turnover or activation of macropinocytosis through ruffling. Membrane ruffling has been extensively studied in the field of cationic cell penetrating peptides [14, 30]. In the present study we found that the cellular uptake of the positively charged nanogel (+ 25 mV)[16], was significantly affected in Pak-1 depleted cells (Figure 5, A and B).

Studies using chemical inhibitors in HeLa cells have suggested that macropinocytosis plays a crucial role in the internalisation of hydrophobically modified glycol chitosan nanoparticles (mean size 350 nm and positive surface charge, + 22 mV) [4]. However, other uptake pathways were also thought to be involved in uptake of these nanoparticles.

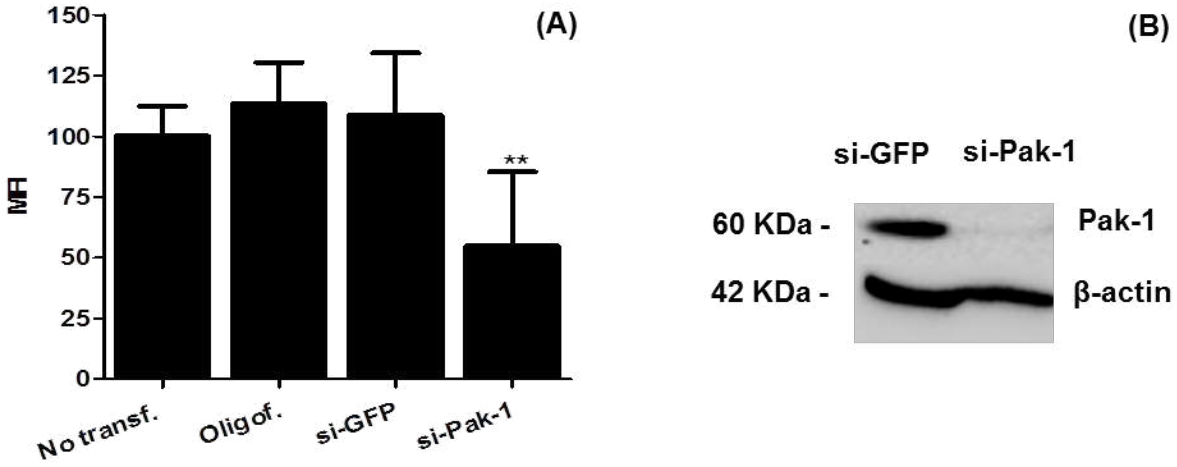

Figure 5. Pak-1 depletion of HeLa cells. (A) Inhibition of nanogel cellular uptake, expressed as mean fluorescence intensity (MFI). ** represents statistical significance of $p< 0.01$ for differences in nanogel uptake between untransfected cells and si-Pak-1 transfected cells, error bars represent S.D.; (B) Pak-1 expression after transfecting HeLa cells for 48 h with control or si-Pak-1.

Inhibition of clathrin- and caveolin-independent endocytosis: Cdc42 and flotillin dependent endocytosis

Nanoparticles and polymers modified with folate have been shown to bind to folate receptors that are often over-expressed in tumour cells [6, 32]. These multiple glycophosphatidylinositol-anchored proteins (GPI-Aps) are slowly internalised by cells and can be detected in a population of early endosomal organelles referred to as GPI-enriched early endosomal compartments, or GEECs. The uptake process is not blocked by perturbations of CME [26, 31]. Cdc42-dependent endocytosis has been reported to be involved in the uptake of GPI-anchored proteins [23], and due to the actin mediated effects of Cdc42 it is also a well characterised regulator of macropinocytosis [29]. Raft-associated proteins flotillin -1 and flotillin-2 are also thought to play a

role in cellular uptake and trafficking mechanisms of nanoparticles. Flotillin-1 has been described as regulator of specific clathrin and caveolae-independent uptake mechanisms [15, 23]. Furthermore, flotillins appear to play a general function in late- or lysosomal degradation or storage processes [33].

In order to investigate whether the nanogel internalisation is affected by flotillin-1 and/or Cdc42-dependent pathways, expression of these proteins in HeLa cells was siRNA-depleted prior to performing uptake assays. The results shown in Figure 6 (A) demonstrate that cellular uptake is significantly affected in these endocytosis compromised cells: nanogel uptake was inhibited by approximately 70% and 65% in cells depleted of flotillin-1 (Figure 6, B) or Cdc42, respectively. We are currently unable to label Cdc42 on membranes to investigate the extent of protein depletion but importantly, two different sequences targeting Cdc42 were shown to have almost identical effects on nanogel uptake.

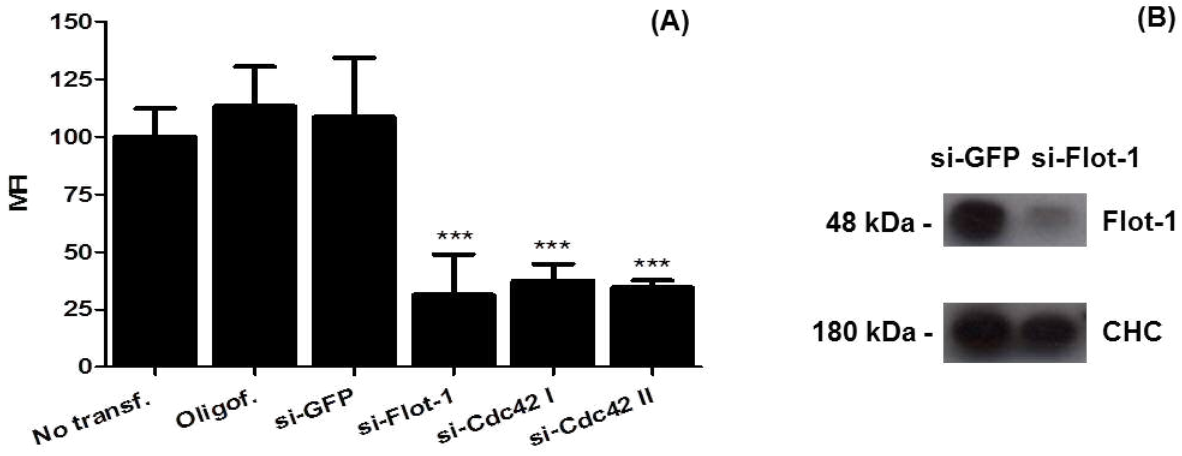

Figure 6. (A) Flow cytometry analysis of the HeLa cells depleted of flot-1 or Cdc42 and incubated with Alexa488-nanogel by 7 h. Error bars represent S.D. *** indicates a statistical significance of $p<0.001$ for the differences in nanogel uptake between untransfected cells and the siRNA transfected cells. Error bars represent S.D.; (B) Flotillin-1 expression after transfecting

HeLa cells for 48 h with siRNA targeting Flot-1. CHC expression was measured as a loading control.

The complete siRNA data presented in this study are summarised in Figure 7, highlighting that the nanogel internalisation appears to be dependent on multiple endocytic pathways. This has been previously reported for chitosan and chitosan derived nanoparticles using chemical inhibitors of endocytosis [13, 34]. It remains to be determined whether the nanogel is actually entering via a flotillin or Cdc42 mediated pathway or even macropinocytosis, but it raises interesting questions regarding the effect of depletion of these proteins on the overall organisation of the plasma membrane. The effects of depletion of Cdc42 and Pak-1 also highlight the importance of the actin cytoskeleton and most probably macropinocytosis in the uptake of the nanogels. We suggest that nanogels enter the cell through their activation of the cell membrane, promoting their own uptake via actin reorganisation and membrane ruffling. Further experiments are required to test this hypothesis more thoroughly.

Using siRNA to overcome the lack of specificity associated with traditional chemical inhibitors, we are able to more accurately target endocytic pathways utilised by the nanogel. Different pathways can be utilised to direct cargo to various cellular destinations including the lysosomes, Golgi or exocytic structures for recycling. Overall, determining the uptake mechanism utilised by a nanoparticle can significantly aid in the understanding of the nanoparticle's ability to perform its function and provide information for rational design of improved delivery systems.

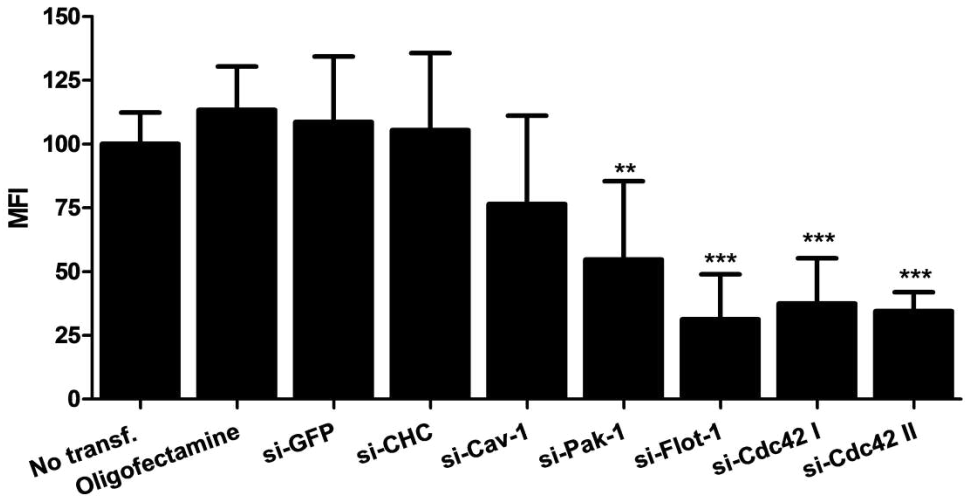

Figure 7. Mean fluorescence intensity (MFI) of the nanogel internalised by HeLa cells transfected with si-CHC, si-Cav-1, si-Pak-1, si-Flot-1 and si-Cdc42, measured by flow cytometry. Untreated cells, cells incubated with oligofectamine alone or transfected with oligofectamine/si-GFP were tested as negative controls. 48 h post transfection the cells were incubated with nanogel, trypsinised and analysed by flow cytometry. ** $p<0.01$ or *** $p<0.001$ represent the statistical significance of differences in nanogel between untransfected cells and the remaining samples. Error bars represent S.D.

3.3. Nanogel intracellular localisation

Once the key mechanisms of nanogel internalisation had been identified, we aimed to investigate their intracellular fate by confocal laser scanning microscopy. Determining the subcellular localisation of these vectors at different time points can give important information regarding their suitability for delivering therapeutic cargo into cells and specific subcellular compartments. For this, we made use of well-characterised endocytic probes whose mechanism of uptake is understood, as is their eventual cellular fate. The intracellular localisation of the Alexa488-nanogel was compared with transferrin and dextran, both labelled with Alexa647. By using

specific experimental conditions, these probes can be used to identify early, recycling and late endosomes as well as terminal lysosomes [21, 35].

When internalised, iron loaded holo-transferrin is trafficked via clathrin coated vesicles to early endosomes and then further directed to recycling endosomes, Finally, it is returned to the cell surface as apo-transferrin for another constitutive cycle of iron loading [21]. To determine if the nanogels enter the same early/recycling endosomal compartment as transferrin we co-incubated the two compounds for the final 16 min of the 7 h nanogel uptake period prior to performing live cell confocal microscopy. This short period allows the transferrin to traffic to, and so label, early and recycling endosomes. The images and colocalisation data shown in Figure 8 (A-C) demonstrate that there is very little colocalisation between transferrin and the nanogel after they have entered the cell. This is expected based on data in Figure 3 and also the possibility that most of the nanogels have trafficked to other endocytic compartments that would be devoid of transferrin labelling, i.e. late endosomes and lysosomes.

To test whether the nanogel was in fact being trafficked via endolysosomal structures, nanogel/dextran co-incubation experiments were performed. These experiments revealed considerable colocalisation (~50%) between nanogel and dextran, as illustrated by co-localisation of the two probes in distinct intracellular yellow dots Figure 8 (D-F).

Cdc42 has also been shown to regulate fluid phase endocytosis and dextran enters cells via this mechanism [36]. Thus the inference from the data in Figure 8F, would be that the nanogel colocalised with the dextran represents the fraction of nanogel that enter the cell in a Cdc42 dependent manner. This conclusion is strengthened by our findings in Figure 6 that Cdc42 is required for ~70% of nanogel uptake. The absence of complete colocalisation may be attributed to the fraction that enters the cell via lipid rafts and regulated by expression of flot-1. Previous

studies by other researchers have demonstrated a high extent of colocalisation between acidic organelles and hydrophobically modified glycol chitosan nanoparticles in HeLa H2B-GFP cells labelled with LysoTracker© Red probe [4]. Other research using human renal proximal tubular KHC cells has shown that 50 % of positively charged chitosan based nanoparticles could escape from lysosomes and reach the cytosol, after 6 h of incubation [37]. Lower levels of colocalisation (~20%) of hydrophobically modified glycol chitosan nanoparticles/lysosomal vesicles labelled with LysoTracker© in HeLa cells has also been noted [34].

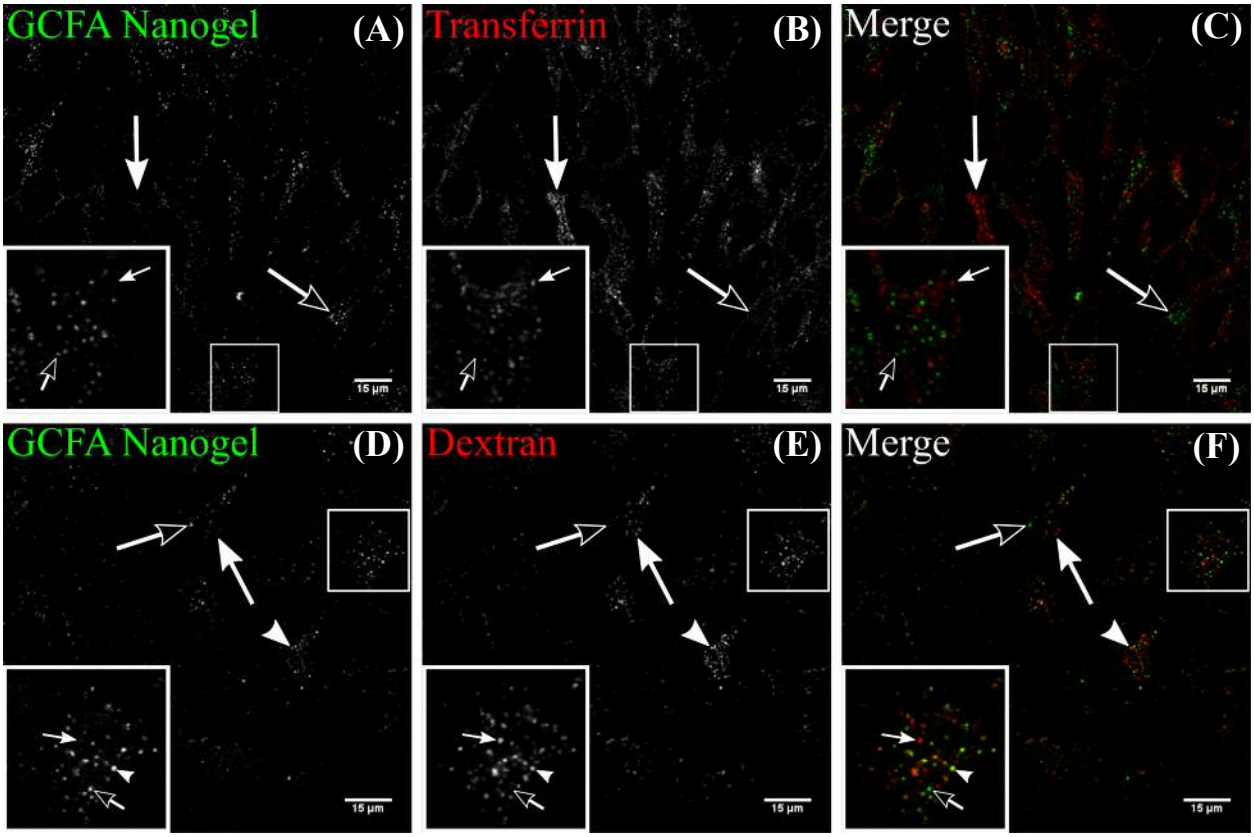

Figure 8. Nanogel subcellular distribution in HeLa cells after 7h of incubation with (A-C) Alexa647-transferrin (16 min prior to analysis) or (D-F) Alexa647-Dextran (7 h co-incubation). The images correspond to single channel capture of nanogels (A,D, green in merge) transferrin (B, red in merge) and Dextran (E, red in merge) and respective merged images (C, F) Unfilled

arrows show single nanogel structures, filled arrows show single transferrin or dextran structures and arrowheads show colocalisation between nanogel and probe. Scale bars represent 15 μm.

The data from this study suggest that a fraction of nanogel may ultimately be delivered to lysosomes. This is not unexpected as pathways such as CME, caveolae and macropinocytosis have been shown to deliver some ligands and their receptors to lysosomes. However, because molecules such as transferrin can enter cells via CME but are recycled rather than degraded it remains to be determined what, if any, fraction of the nanogels recycles. The possibility exists that recycling could be mediated from late endocytic structures via a pathway that may be distinct from that used by transferrin.[38]

Although undesirable in many cases for therapeutic cargo that would be inactivated in lysosomes e.g. siRNA or DNA, specific lysosome targeting may be beneficial for drug delivery strategies to replace deficient lysosome enzymes to treat conditions such as lysosomal storage diseases [39]. Beyond this, nanomedicines targeting the endolysosomal pathway also have potential for improving drug delivery to address other major disease burdens including Alzheimer Disease and cancer [3, 37].

4. Conclusions

Inhibition of endocytic pathways via siRNA depletion of specific endocytic proteins has provided new insights into the way that nanogel enters cells with respect to the requirements for specific proteins and the types of pathways that they orchestrate.

The involvement of Cdc42 and Pak-1 strongly suggest that actin reorganisation is also required for uptake but whether this is constitutive or active macropinocytosis remains to be determined.

Colocalisation studies with endocytic probes showed that some of nanogel is delivered to endolysosomal compartments but a significant fraction was also in organelles that await further characterisation.

Supporting Information available.

Live cell confocal microscopy observation of Alexa488-nanogels incubated with si-CHC and si-Cav-1 transfected cells. This material is available free of charge via the Internet at http://pubs.acs.org."

AUTHOR INFORMATION

Corresponding Author

Francisco M. Gama*

Centre of Biological Engineering, University of Minho, Campus the Gualtar, 4710-057 Braga, Portugal;

fmgama@deb.uminho.pt

ACKNOWLEDGMENT

The authors (PP, FMG) thank the Project "BioHealth - Biotechnology and Bioengineering approaches to improve health quality", Ref. NORTE-07-0124-FEDER-000027, co-funded by the Programa Operacional Regional do Norte (ON.2 – O Novo Norte), QREN, FEDER. PP was funded through FCT Ph.D. grant ref SFRH/BD/64977/2009. Funding is also acknowledged from a Cancer Research UK studentship (C36040/A11652) to ATJ, JMW and EPSRC Grant EP/J021334/1 (ATJ, EJS).

REFERENCES

1. Gao, H.; Yang, Z.; Zhang, S.; Cao, S.; Shen, S.; Pang, Z.; Jiang, X. Ligand modified nanoparticles increases cell uptake, alters endocytosis and elevates glioma distribution and internalization. *Sci. Rep.* **2013,** *3*.
2. Harush-Frenkel, O.; Debotton, N.; Benita, S.; Altschuler, Y. Targeting of nanoparticles to the clathrin-mediated endocytic pathway. *Biochemical and biophysical research communications* **2007,** *353*, (1), 26-32.
3. Bareford, L. M.; Swaan, P. W. Endocytic mechanisms for targeted drug delivery. *Advanced drug delivery reviews* **2007,** *59*, (8), 748-58.
4. Park, S.; Lee, S. J.; Chung, H.; Her, S.; Choi, Y.; Kim, K.; Choi, K.; Kwon, I. C. Cellular uptake pathway and drug release characteristics of drug-encapsulated glycol chitosan nanoparticles in live cells. *Microscopy research and technique* **2010,** *73*, (9), 857-65.
5. Doherty, G. J.; McMahon, H. T. Mechanisms of endocytosis. *Annual review of biochemistry* **2009,** *78*, 857-902.
6. Sahay, G.; Alakhova, D. Y.; Kabanov, A. V. Endocytosis of nanomedicines. *Journal of controlled release : official journal of the Controlled Release Society* **2010,** *145*, (3), 182-95.
7. Xu, S.; Olenyuk, B. Z.; Okamoto, C. T.; Hamm-Alvarez, S. F. Targeting receptor-mediated endocytotic pathways with nanoparticles: rationale and advances. *Advanced drug delivery reviews* **2013,** *65*, (1), 121-38.
8. Xiang, S.; Tong, H.; Shi, Q.; Fernandes, J. C.; Jin, T.; Dai, K.; Zhang, X. Uptake mechanisms of non-viral gene delivery. *Journal of controlled release : official journal of the Controlled Release Society* **2012,** *158*, (3), 371-8.
9. Ilina, P.; Hyvonen, Z.; Saura, M.; Sandvig, K.; Yliperttula, M.; Ruponen, M. Genetic blockage of endocytic pathways reveals differences in the intracellular processing of non-viral gene delivery systems. *Journal of controlled release : official journal of the Controlled Release Society* **2012,** *163*, (3), 385-95.
10. Wang, X.; Yao, S.; Ahn, H.-Y.; Zhang, Y.; Bondar, M. V.; Torres, J. A.; Belfield, K. D., *Folate receptor targeting silica nanoparticle probe for two-photon fluorescence bioimaging*. 2010; Vol. 1, p 453-462.
11. Vercauteren, D.; Vandenbroucke, R. E.; Jones, A. T.; Rejman, J.; Demeester, J.; De Smedt, S. C.; Sanders, N. N.; Braeckmans, K. The use of inhibitors to study endocytic pathways of gene carriers: optimization and pitfalls. *Molecular therapy : the journal of the American Society of Gene Therapy* **2010,** *18*, (3), 561-9.
12. Ivanov, A. I. Pharmacological inhibition of endocytic pathways: is it specific enough to be useful? *Methods in molecular biology (Clifton, N.J.)* **2008,** *440*, 15-33.
13. Garaiova, Z.; Strand, S. P.; Reitan, N. K.; Lelu, S.; Storset, S. O.; Berg, K.; Malmo, J.; Folasire, O.; Bjorkoy, A.; Davies Cde, L. Cellular uptake of DNA-chitosan nanoparticles: the role of clathrin- and caveolae-mediated pathways. *International journal of biological macromolecules* **2012,** *51*, (5), 1043-51.
14. Al Soraj, M.; He, L.; Peynshaert, K.; Cousaert, J.; Vercauteren, D.; Braeckmans, K.; De Smedt, S. C.; Jones, A. T. siRNA and pharmacological inhibition of endocytic pathways to characterize the differential role of macropinocytosis and the actin cytoskeleton on cellular

uptake of dextran and cationic cell penetrating peptides octaarginine (R8) and HIV-Tat. *Journal of controlled release : official journal of the Controlled Release Society* **2012,** *161*, (1), 132-41.
15. Vercauteren, D.; Piest, M.; van der Aa, L. J.; Al Soraj, M.; Jones, A. T.; Engbersen, J. F.; De Smedt, S. C.; Braeckmans, K. Flotillin-dependent endocytosis and a phagocytosis-like mechanism for cellular internalization of disulfide-based poly(amido amine)/DNA polyplexes. *Biomaterials* **2011,** *32*, (11), 3072-84.
16. Pereira, P.; Morgado, D.; Crepet, A.; David, L.; Gama, F. M. Glycol chitosan-based nanogel as a potential targetable carrier for siRNA. *Macromolecular bioscience* **2013,** *13*, (10), 1369-78.
17. Mosmann, T. Rapid colorimetric assay for cellular growth and survival: Application to proliferation and cytotoxicity assays. *Journal of Immunological Methods* **1983,** *65*, (1–2), 55-63.
18. Papazisis, K. T.; Geromichalos, G. D.; Dimitriadis, K. A.; Kortsaris, A. H. Optimization of the sulforhodamine B colorimetric assay. *Journal of immunological methods* **1997,** *208*, (2), 151-8.
19. Skehan, P.; Storeng, R.; Scudiero, D.; Monks, A.; McMahon, J.; Vistica, D.; Warren, J. T.; Bokesch, H.; Kenney, S.; Boyd, M. R. New colorimetric cytotoxicity assay for anticancer-drug screening. *Journal of the National Cancer Institute* **1990,** *82*, (13), 1107-12.
20. Liu, L.; Zheng, M.; Renette, T.; Kissel, T. Modular Synthesis of Folate Conjugated Ternary Copolymers: Polyethylenimine-graft-Polycaprolactone-block-Poly(ethylene glycol)-Folate for Targeted Gene Delivery. *Bioconjugate Chemistry* **2012,** *23*, (6), 1211-1220.
21. Mayle, K. M.; Le, A. M.; Kamei, D. T. The intracellular trafficking pathway of transferrin. *Biochimica et biophysica acta* **2012,** *1820*, (3), 264-81.
22. Chiu, Y. L.; Ho, Y. C.; Chen, Y. M.; Peng, S. F.; Ke, C. J.; Chen, K. J.; Mi, F. L.; Sung, H. W. The characteristics, cellular uptake and intracellular trafficking of nanoparticles made of hydrophobically-modified chitosan. *Journal of controlled release : official journal of the Controlled Release Society* **2010,** *146*, (1), 152-9.
23. Sandvig, K.; Pust, S.; Skotland, T.; van Deurs, B. Clathrin-independent endocytosis: mechanisms and function. *Current Opinion in Cell Biology* **2011,** *23*, (4), 413-420.
24. Dauty, E.; Remy, J. S.; Zuber, G.; Behr, J. P. Intracellular delivery of nanometric DNA particles via the folate receptor. *Bioconjug Chem* **2002,** *13*, (4), 831-9.
25. Turek, J. J.; Leamon, C. P.; Low, P. S. Endocytosis of folate-protein conjugates: ultrastructural localization in KB cells. *Journal of cell science* **1993,** *106 (Pt 1)*, 423-30.
26. Sabharanjak, S.; Sharma, P.; Parton, R. G.; Mayor, S. GPI-anchored proteins are delivered to recycling endosomes via a distinct cdc42-regulated, clathrin-independent pinocytic pathway. *Developmental cell* **2002,** *2*, (4), 411-23.
27. Iversen, T.-G.; Skotland, T.; Sandvig, K. Endocytosis and intracellular transport of nanoparticles: Present knowledge and need for future studies. *Nano Today* **2011,** *6*, (2), 176-185.
28. Peng, S. F.; Tseng, M. T.; Ho, Y. C.; Wei, M. C.; Liao, Z. X.; Sung, H. W. Mechanisms of cellular uptake and intracellular trafficking with chitosan/DNA/poly(gamma-glutamic acid) complexes as a gene delivery vector. *Biomaterials* **2011,** *32*, (1), 239-48.
29. Kerr, M. C.; Teasdale, R. D. Defining macropinocytosis. *Traffic (Copenhagen, Denmark)* **2009,** *10*, (4), 364-71.
30. Jones, A. T. Macropinocytosis: searching for an endocytic identity and role in the uptake of cell penetrating peptides. *Journal of cellular and molecular medicine* **2007,** *11*, (4), 670-84.
31. Hansen, C. G.; Nichols, B. J. Molecular mechanisms of clathrin-independent endocytosis. *Journal of cell science* **2009,** *122*, (Pt 11), 1713-21.

32. Lu, Y.; Low, P. S. Folate-mediated delivery of macromolecular anticancer therapeutic agents. *Advanced drug delivery reviews* **2002,** *54*, (5), 675-93.
33. Kasper, J.; Hermanns, M. I.; Bantz, C.; Utech, S.; Koshkina, O.; Maskos, M.; Brochhausen, C.; Pohl, C.; Fuchs, S.; Unger, R. E.; Kirkpatrick, C. J. Flotillin-involved uptake of silica nanoparticles and responses of an alveolar-capillary barrier in vitro. *European journal of pharmaceutics and biopharmaceutics : official journal of Arbeitsgemeinschaft fur Pharmazeutische Verfahrenstechnik e.V* **2013,** *84*, (2), 275-87.
34. Nam, H. Y.; Kwon, S. M.; Chung, H.; Lee, S. Y.; Kwon, S. H.; Jeon, H.; Kim, Y.; Park, J. H.; Kim, J.; Her, S.; Oh, Y. K.; Kwon, I. C.; Kim, K.; Jeong, S. Y. Cellular uptake mechanism and intracellular fate of hydrophobically modified glycol chitosan nanoparticles. *Journal of controlled release : official journal of the Controlled Release Society* **2009,** *135*, (3), 259-67.
35. Pangarkar, C.; Dinh, A. T.; Mitragotri, S. Endocytic pathway rapidly delivers internalized molecules to lysosomes: an analysis of vesicle trafficking, clustering and mass transfer. *Journal of controlled release : official journal of the Controlled Release Society* **2012,** *162*, (1), 76-83.
36. Cheng, Z. J.; Singh, R. D.; Holicky, E. L.; Wheatley, C. L.; Marks, D. L.; Pagano, R. E. Co-regulation of caveolar and Cdc42-dependent fluid phase endocytosis by phosphocaveolin-1. *The Journal of biological chemistry* **2010,** *285*, (20), 15119-25.
37. Yue, Z.-G.; Wei, W.; Lv, P.-P.; Yue, H.; Wang, L.-Y.; Su, Z.-G.; Ma, G.-H. Surface Charge Affects Cellular Uptake and Intracellular Trafficking of Chitosan-Based Nanoparticles. *Biomacromolecules* **2011,** *12*, (7), 2440-2446.
38. Grant, B. D.; Donaldson, J. G. Pathways and mechanisms of endocytic recycling. *Nat Rev Mol Cell Biol* **2009,** *10*, (9), 597-608.
39. Desnick, R. J.; Schuchman, E. H. Enzyme replacement therapy for lysosomal diseases: lessons from 20 years of experience and remaining challenges. *Annual review of genomics and human genetics* **2012,** *13*, 307-35.

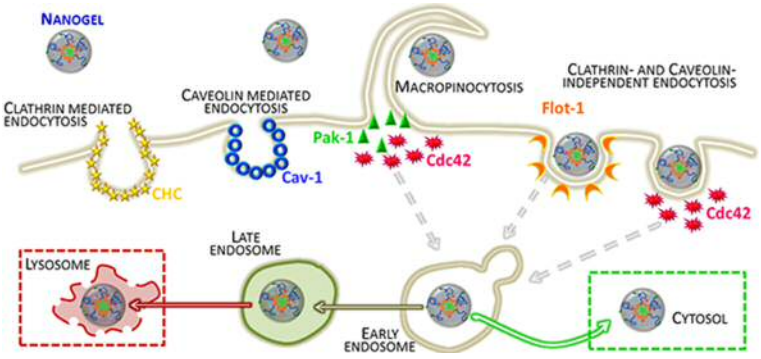

Endocytic pathways and endocytic proteins regulating the uptake of therapeutic macromolecules. Broken arrows highlight nanogel uptake pathways.